

# Stabilization of counterpropagating solitons by photonic lattices

Sebastian Koke<sup>1</sup>, Denis Träger<sup>1</sup>, Philip Jander<sup>1</sup>, Michael Chen<sup>2</sup>,  
Dragomir N. Neshev<sup>2</sup>, Wieslaw Krolikowski<sup>2</sup>, Yuri S. Kivshar<sup>2</sup>,  
and Cornelia Denz<sup>1\*</sup>

<sup>1</sup> *Institut für Angewandte Physik and Center for Nonlinear Science (CeNoS), Westfälische Wilhelms-Universität, 48149 Münster, Germany*

<sup>2</sup> *Nonlinear Physics Centre and Laser Physics Centre, Centre for Ultrahigh-bandwidth Devices for Optical Systems (CUDOS), Research School of Physical Sciences and Engineering, Australian National University, Canberra, ACT 0200, Australia*

\* *Corresponding author: [denz@uni-muenster.de](mailto:denz@uni-muenster.de)*

**Abstract:** We report on the stabilization of inherently unstable counterpropagating photorefractive spatial solitons by the use of one- and two-dimensional photonic lattices. We numerically investigate the dependence of the instability dynamics on period and amplitude of the lattice and present experimental verification for the dynamic stabilization of the bi-directional soliton state.

© 2007 Optical Society of America

**OCIS codes:** 190.4420: Transverse effects in nonlinear optics; 190.5330: Photorefractive nonlinear optics; 190.5530: Pulse propagation and solitons

---

## References and links

1. G. I. Stegeman and M. Segev, "Optical Spatial Solitons and Their Interactions: Universality and Diversity," *Science* **286**, 1518–1523 (1999).
2. W. Krolikowski, B. Luther-Davies, and C. Denz, "Photorefractive Solitons," *IEEE J. Sel. Top. Quantum Electron.* **39**, 3–12 (2003).
3. Y. S. Kivshar and G. P. Agrawal, *Optical Solitons: From Fibers to Photonic Crystals* (Academic Press, San Diego, 2003).
4. D. Träger, N. Sagemerten, and C. Denz, "Guiding of Dynamically Modulated Signals in Arrays of Photorefractive Spatial Solitons," *IEEE J. Sel. Top. Quantum Electron.* **12**, 383–387 (2006).
5. C. Weillnau, M. Ahles, J. Petter, D. Träger, J. Schröder, and C. Denz, "Spatial optical (2+1)-dimensional scalar- and vector-solitons in saturable nonlinear media," *Ann. Phys.* **11**, 573–629 (2002).
6. O. Cohen, R. Uzdin, T. Carmon, J. W. Fleischer, M. Segev, and S. Odoulov, "Collisions between Optical Spatial Solitons Propagating in Opposite Directions," *Phys. Rev. Lett.* **89**, 133,901–4 (2002).
7. D. Kip, C. Herden, and M. Wesner, "All-Optical Signal Routing Using Interaction of Mutually Incoherent Spatial Solitons," *Ferroelectrics* **274**, 135–142 (2002).
8. P. Jander, J. Schröder, C. Denz, M. Petrovic, and M. R. Belic, "Dynamic instability of self-induced bidirectional waveguides in photorefractive media," *Opt. Lett.* **30**, 750–752 (2005).
9. K. Motzek, P. Jander, A. Desyatnikov, M. Belic, C. Denz, and F. Kaiser, "Dynamic counterpropagating vector solitons in saturable self-focusing media," *Phys. Rev. E* **68**, 066,611–4 (2003).
10. M. R. Belic, P. Jander, A. Strinic, A. Desyatnikov, and C. Denz, "Self-trapped bidirectional waveguides in a saturable photorefractive medium," *Phys. Rev. E* **68**, R025,601–4 (2003).
11. M. Belic, P. Jander, K. Motzek, A. Desyatnikov, D. Jovic, A. Strinic, M. Petrovic, C. Denz, and F. Kaiser, "Counterpropagating self-trapped beams in photorefractive crystals," *J. Opt. B* **6**, S190–S196 (2004).
12. P. Jander, J. Schröder, T. Richter, K. Motzek, F. Kaiser, M. R. Belic, and C. Denz, "Dynamic instability of counterpropagating self-trapped beams in photorefractive media," *Proc. SPIE* **6255**, 62,550A (2006).
13. M. Haelterman, A. P. Sheppard, and A. W. Snyder, "Bimodal counterpropagating spatial solitary-waves," *Opt. Commun.* **103**, 145–152 (1993).

14. Y. Silberberg and I. B. Joseph, "Instabilities, Self-Oscillation, and Chaos in a Simple Nonlinear Optical Interaction," *Phys. Rev. Lett.* **48**, 1541–1543 (1982). URL <http://link.aps.org/abstract/PRL/v48/p1541>.
15. W. J. Firth and C. Pare, "Transverse modulational instabilities for counterpropagating beams in Kerr media," *Opt. Lett.* **13**, 1096 (1988).
16. W. J. Firth, A. Fitzgerald, and C. Pare "Transverse instabilities due to counterpropagation in Kerr media," *J. Opt. Soc. Am. B* **7**, 1087–1097 (1990).
17. F. T. Arecchi, S. Boccaletti, and P. Ramazza, "Pattern formation and competition in nonlinear optics," *Phys. Rep.* **318**, 1–83 (1999).
18. O. Cohen, S. Lan, T. Carmon, J. A. Giordmaine, and M. Segev, "Spatial vector solitons consisting of counter-propagating fields," *Opt. Lett.* **27**(22), 2013 (2002).
19. D. N. Christodoulides, F. Lederer, and Y. Silberberg, "Discretizing light behaviour in linear and nonlinear waveguide lattices," *Nature* **424**, 817–823 (2003).
20. A. L. Jones, "Coupling of optical fibers and scattering in fibers," *J. Opt. Soc. Am.* **55**, 261–271 (1965).
21. S. Somekh, E. Gamire, A. Yariv, H. L. Garvin, and R. G. Hunsperger, "Channel optical waveguide directional couplers," *Appl. Phys. Lett.* **22**, 46–48 (1973).
22. D. N. Christodoulides and R. I. Joseph, "Discrete self-focusing in nonlinear arrays of coupled waveguides," *Opt. Lett.* **13**, 794–796 (1988).
23. N. K. Efremidis, S. Sears, D. N. Christodoulides, J. W. Fleischer, and M. Segev, "Discrete solitons in photorefractive optically induced photonic lattices," *Phys. Rev. E* **66**, 046,602–5 (2002).
24. H. S. Eisenberg, Y. Silberberg, R. Morandotti, A. R. Boyd, and J. S. Aitchison, "Discrete spatial optical solitons in waveguide arrays," *Phys. Rev. Lett.* **81**(16), 3383–3386 (1998). URL <http://link.aps.org/abstract/PRL/v81/p3383>.
25. J. W. Fleischer, T. Carmon, M. Segev, N. K. Efremidis, and D. N. Christodoulides, "Observation of discrete solitons in optically induced real time waveguide arrays," *Phys. Rev. Lett.* **90**(2), 023,902–4 (2003). URL <http://link.aps.org/abstract/PRL/v90/p023902>.
26. J. W. Fleischer, M. Segev, N. K. Efremidis, and D. N. Christodoulides, "Observation of two-dimensional discrete solitons in optically induced nonlinear photonic lattices," *Nature* **422**, 147–150 (2003).
27. D. Neshev, E. A. Ostrovskaya, Y. Kivshar, and W. Krolikowski, "Spatial solitons in optically induced gratings," *Opt. Lett.* **28**, 710–712 (2003).
28. D. Mandelik, R. Morandotti, J. S. Aitchison, and Y. Silberberg, "Gap solitons in waveguide arrays," *Phys. Rev. Lett.* **92**(9), 093,904–4 (2004). URL <http://link.aps.org/abstract/PRL/v92/p093904>.
29. D. Neshev, A. A. Sukhorukov, B. Hanna, W. Krolikowski, and Y. S. Kivshar, "Controlled generation and steering of spatial gap solitons," *Phys. Rev. Lett.* **93**(8), 083,905–4 (2004). URL <http://link.aps.org/abstract/PRL/v93/p083905>.
30. E. Smirnov, M. Stepic, C. Ruter, V. Shandarov, and D. Kip, "Interaction of counterpropagating discrete solitons in a nonlinear one-dimensional waveguide array," *Opt. Lett.* **32**, 512–514 (2007).
31. M. Segev, G. C. Valley, B. Crosignani, P. DiPorto, and A. Yariv, "Steady-State Spatial Screening Solitons in Photorefractive Materials with External Applied Field," *Phys. Rev. Lett.* **73**, 3211–3214 (1994).
32. L. Solymar, D. J. Webb, and A. Grunnett-Jepsen, *The Physics of Photorefractive Materials*, 2nd ed. (Clarendon Press, Oxford, 1996).
33. M. Carvalho, S. Singh, and D. Christodoulides, "Self-deflection of steady-state bright spatial solitons in biased photorefractive crystals," *Opt. Commun.* **120**(5), 311–315 (1995).
34. M. Shih, M. Segev, G. Valley, G. Salomono, B. Crosignani, and P. DiPorto, "Observation of two-dimensional steady-state photorefractive screening solitons," *Electron. Lett.* **31**(10), 826–828 (1995).
35. C. Rotschild, O. Cohen, O. Manela, T. Carmon, and M. Segev, "Interactions between spatial screening solitons propagating in opposite directions," *J. Opt. Soc. Am. B* **21**, 1354–1357 (2004). URL <http://www.opticsinfobase.org/abstract.cfm?URI=josab-21-7-1354>.
36. W. Krolikowski, M. Saffman, B. Luther-Davies, and C. Denz, "Anomalous Interaction of Spatial Solitons in Photorefractive Media," *Phys. Rev. Lett.* **80**, 3240–3243 (1998).
37. G. P. Agrawal, *Nonlinear Fiber Optics*, 2nd ed. (Academics Press, San Diego, 1995).
38. J. B. Geddes, R. A. Indik, J. V. Moloney, and W. J. Firth, "Hexagons and squares in a passive nonlinear optical system," *Phys. Rev. A* **50**, 3471–3485, (1994).
39. M. Litzkow, M. Livny, and M. Mutka, "Condor - A Hunter of Idle Workstations," in *ICDCS*, pp. 104–111 (IEEE-CS Press, 1988). URL <http://www.cs.wisc.edu/condor/>.
40. R. Fischer, D. Träger, D. N. Neshev, A. A. Sukhorukov, W. Krolikowski, C. Denz, and Y. S. Kivshar, "Reduced-symmetry two-dimensional solitons in photonic lattices," *Phys. Rev. Lett.* **96**(2), 023,905–4 (2006). URL <http://link.aps.org/abstract/PRL/v96/p023905>.
41. D. Träger, R. Fischer, D. N. Neshev, A. A. Sukhorukov, C. Denz, W. Krolikowski, and Y. S. Kivshar, "Nonlinear Bloch modes in two-dimensional photonic lattices," *Opt. Express* **14**(5), 1913–1923 (2006). URL <http://www.opticsinfobase.org/abstract.cfm?URI=oe-14-5-1913>.

## 1. Introduction

The formation of self-trapped beams in nonlinear optical media, commonly referred to as spatial optical solitons, has gained much interest in recent years [1–3] mainly because of the soliton's waveguiding capabilities [4]. Due to the reversibility of the process of light-induced refractive index modulations spatial optical solitons offer potential application in future reconfigurable optical links, exploiting the light-guiding-light concept. For such devices, the interaction of spatial optical solitons is of crucial importance. It turns out that the interaction scenarios strongly depend on the particularities of the nonlinear response of actual material. In the case of, for instance, photorefractive solitons the interactions can include attraction or repulsion as well as energy exchange and fusion or even a creation of new solitons [1,2]. Prior studies were mainly concerned with the interaction of *co-propagating* solitons [5]. With such one-sided boundary conditions, a temporally constant input generally leads to a stationary state after initial transient dynamics. In contrast, the boundary conditions of *counter-propagating* [6–13] solitons are partially fixed at opposite crystal faces. Generally, optical counterpropagation in nonlinear optical media is known to lead to various spatial and temporal instabilities and related phenomena such as pattern formation [14–17]. Recently, numerical simulations [9–12] revealed two instability regimes depending on the strength of the nonlinear interaction parameter  $\Gamma L$ , where  $\Gamma$  is the photorefractive coupling constant and  $L$  the medium length. The first one is marked by the break-up of the stationary soliton-induced common waveguide observed for low coupling strengths into a so-called bidirectional waveguide structure in the form of spatially interlaced (interweaved) channels [9, 10, 18]. This new waveguide still represents a steady state structure and is similar to the one observed earlier in Kerr media [13]. For even stronger nonlinear coupling the bidirectional waveguide loses stability via regular limit-cycle oscillations until the temporal dynamics becomes irregular [12] as was also demonstrated experimentally [8].

For practical applications, e.g. as self-aligning optical links, such oscillations are obviously undesired. Therefore, ways to control and stabilize counterpropagating solitons have to be found. In this work we present a novel approach to suppress the instability of counterpropagating solitons by using an optically-induced photonic lattice inside the photorefractive crystal. The periodic modulation of the refractive index of the material imposed by the lattice affects fundamental properties of light propagation inside the medium. The modulation acts as a periodic potential, reducing the spatial mobility of optical beams and enabling the formation of lattice solitons in the total internal reflection gap. Subsequently, this is expected to suppress the instability of the counterpropagating solitons and therefore allowing for stability of the resulting composite waveguide. Here we study numerically the temporal stability of the counterpropagating solitons as a function of strength and period of the optical lattice and demonstrate experimentally the effect of instability arrest by one- (1D) and two-dimensional (2D) optical lattices.

A periodic modulation of the material refractive index imposes a qualitatively new behaviour of light propagation reflecting the discrete nature of the medium [19]. Narrow light beams propagating in the linear regime experience the well known discrete diffraction as first predicted theoretically in 1965 [20] and experimentally observed in a Gallium Arsenide waveguide array in 1973 [21]. In a medium with nonlinear optical response, discrete and gap solitons can exist. In case of self-focusing nonlinearity the discrete solitons can be excited from the top of the first band of the lattice bandgap spectrum and exist in the total internal reflection gap [19, 22, 23]. These solitons have been investigated experimentally in AlGaAs waveguide

arrays [24] and optically-induced photonic lattices [25–27]. In contrast, gap solitons in focusing nonlinear medium require excitation from the top of the second band and exist in the finite Bragg reflection gap [28, 29].

Among the various periodic structures used to demonstrate nonlinear localization and soliton formation the optically-induced lattices [23] have attracted special attention. In this case the periodic modulation of the refractive index is optically-induced inside a DC-biased photorefractive crystal by the interference of two or more broad ordinarily polarized beams. Due to the electro-optic anisotropy of the crystal the lattice writing beams are not affected by the applied voltage, while any extraordinarily polarized probe beam will experience periodic index modulation and strong self-action due to the photorefractive effect. In our studies we employed the optically-induced lattice technique to study the dependence of counterpropagating soliton dynamics on the lattice depth and period. Furthermore, the lattice geometry can be changed from 1D to 2D by adding more interference beams, thus enabling study of the instability suppression in two transverse directions. The dynamic tunability of the optical lattice is a great advantage over fabricated permanent structures [30].

In the first part of this paper, we investigate numerically the influence of the lattice period and amplitude on interaction dynamics of counterpropagating photorefractive solitons. Thereafter, we provide experimental demonstration of the theoretically predicted suppression of soliton instability.

## 2. Isotropic one-dimensional model

We investigate the interaction of two counterpropagating mutually incoherent screening solitons [31] by using a one-dimensional model of a saturable nonlinearity. Spatial evolution of the slowly varying field envelopes  $F$  and  $B$  ( $|\partial_z^2 \bullet| \ll |2ik_0 \partial_z \bullet|$ ,  $\partial_t \bullet \simeq 0$ ,  $\partial_t^2 \bullet \simeq 0$  where  $\bullet$  stands for  $F$  and  $B$ , respectively) of the forward and backward propagating beams is modeled in paraxial approximation:

$$\begin{aligned} i\partial_z F + \partial_x^2 F &= \Gamma E^{sc} F \\ -i\partial_z B + \partial_x^2 B &= \Gamma E^{sc} B \end{aligned} \quad (1)$$

where  $E^{sc}$  is the space charge field created by the beams inside the photorefractive crystal and  $\Gamma = k^2 n_0^2 w_0^2 r_{\text{eff}} E_e$  denotes the photorefractive coupling constant, with  $n_0$  being the bulk refractive index,  $r_{\text{eff}}$  the effective coefficient of the electro-optic tensor and  $E_e$  the externally applied electric field necessary for the screening effect to occur. The transverse  $x$ -coordinate is scaled to the beam waist  $w_0$  whereas the propagation  $z$ -coordinate is scaled with the diffraction length  $L_D = 2kw_0^2$ , with  $k = 2\pi n_0/\lambda$  and  $\lambda$  denoting the laser wavelength [10].

For the temporal evolution of the space charge field we assume relaxation type dynamics [32]:

$$\tau(I) \partial_t E^{sc} + E^{sc} = -\frac{I}{1+I}, \quad (2)$$

where  $I = |F|^2 + |B|^2$  is the total intensity scaled to the so-called dark intensity  $I_d$  and  $E^{sc}$  is scaled to  $E_e$ . The relaxation time  $\tau$  depends on the total intensity as  $\tau(I) = \tau_0/(1+I)$  with  $\tau_0$  representing the dark relaxation time constant.

In the above model of the photorefractive effect [Eq.(2)] we neglect diffusion of excited charge carriers inside the crystal. In consequence, we do not account for beam self-bending [33–35]. Additionally, spatial nonlocality causing repulsion of solitary waves propagating at specific relative distances [36] is neglected. While the resulting model serves as an approximation of the real system it nevertheless leads to results which are in a good agreement with experimental observations.

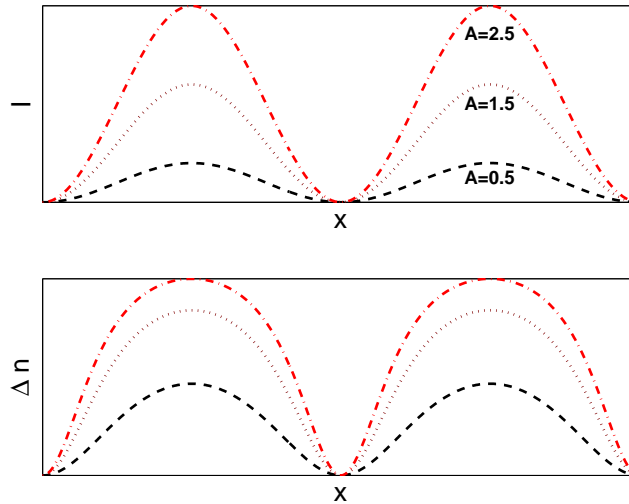


Fig. 1. Steady state modulation of the refractive index (bottom) resulting from lattices with different peak intensities (top) in the applied isotropic model.

The presence of the index grating created by the interference of two plane waves is modeled by including the additional term  $I_{\text{pot}}(x) = A \cos^2(\pi x/p)$  in the expression for the total light intensity  $I = |F|^2 + |B|^2 + I_{\text{pot}}$ , where  $A$  and  $p$  determine the peak intensity and periodicity of the lattice. As the lattice-forming waves are ordinary polarized, they do not interact directly with solitons [23] and the lattice intensity distribution remains stationary throughout the crystal. This lattice intensity pattern and the resulting steady state refractive index modulation are depicted in Fig. 1.

The numerical analysis of the ensuing nonlinear model [Eqs.(1-2)] involves two operations conducted in one discrete time step. At a given time step the propagation of the beams through the medium with a stationary distribution of the space charge field  $E^{\text{sc}}$  is simulated by using a second order split-step Fourier beam propagation method [37, 38]. Thereafter, the temporal evolution of the space charge field as a result of the new intensity distribution is calculated from Eq.(2). The separation of wave propagation from the temporal evolution of the space charge field is reflected in dropping the time derivatives of the field envelopes in the wave equation [Eq.(1)] and is justified due to the large difference in the propagation time ( $10^{-10}$ s) and response time of the photorefractive effect (on the order of  $10^{-3} - 1$ s).

In our investigations we assumed the incident waves to be stationary in a form of two identical Gaussian beams with beam waists 1 and peak intensity  $I = 1$  each. We simulate their head on collision by launching both beams at the same lateral position perpendicularly to the crystal face. The propagation along a crystal of length  $L = 5$  and transverse extension of 20 was calculated on a grid consisting of  $500 \times 512$  grid points. The coupling constant was chosen to be negative ( $\Gamma = -13.2$ ) to ensure the self-focussing regime necessary for the formation of bright solitons. For this set of parameter values the soliton solutions in bulk media already exhibited very irregular temporal oscillations [12]. The numerical simulations started with only the lattice beams present. After evolving the corresponding space charge field over time period  $10\tau_0$  (with the time step of  $0.1\tau_0$ ) we launched both soliton forming beams and simulated the evolution of the whole system over time of  $5000\tau_0$ . The calculations have been carried out on the Morfeus-GRID at the Westfälische Wilhelms-Universität Münster, with the use of Condor [39].

In order to study the influence of the induced photonic lattice on the soliton dynamics we vary

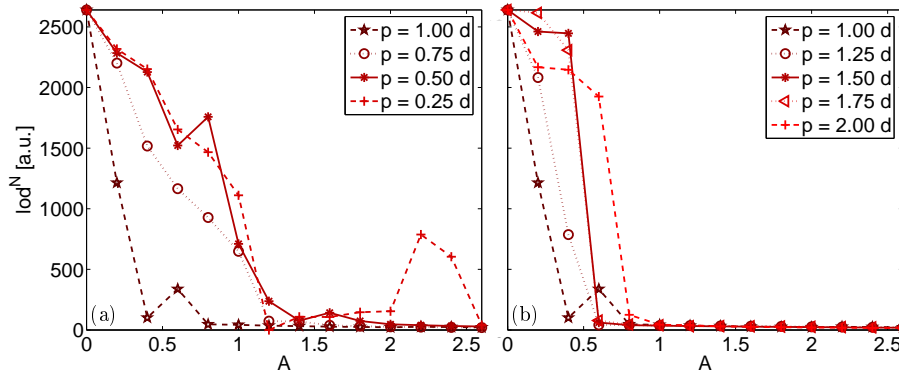


Fig. 2.  $\log^N$  for counterpropagating solitons launched on-site as a function of lattice intensity  $A$  for different lattice periods  $p$ . (a) period smaller than the beam diameter; (b) lattice period larger than the beam diameter. Non-monotonous decrease of  $\log^N$  for  $p = 1d$  and  $A = 0.4 - 0.8$ , is due to long lasting transient dynamics.

the peak intensity and periodicity of the lattice wave and determine the degree of instability in terms of the *level of dynamics* [12] defined as:

$$\log^N = \sum_{t=1}^N \sum_x \left[ \frac{|F(x, L, t) - F(x, L, t-1)|^2}{|F(x, L, t)|^2} + \frac{|B(x, 0, t) - B(x, 0, t-1)|^2}{|B(x, 0, t)|^2} \right] \quad (3)$$

This parameter represents the time and space integrated modulus of the differences in the field envelopes at either exit face between two successive simulated time-steps. It follows directly from Eq.(3) that decrease in the intensity variation of solitons, (i.e. weaker instability) leads to lower value of  $\log^N$  ( $\log^N = 0$  zero for stationary solutions).

As can be clearly seen from Fig. 2 the rate of decrease of the temporal dynamics of counter-propagating solitons launched on-site strongly depends on lattice strength and its period. Here and in the following, on-site denotes the case when the maximum soliton intensity coincides with the maximum of the lattice. The influence on the soliton dynamics is strongest for period  $p = 1d$ , where  $d = 2$  is the beam diameter of the incident Gaussian beams. This can be explained as follows: for small lattice periodicity, the self-trapped beam covers many lattice sites. As a result, the effect of the lattice is weaker, and in the limit  $p \rightarrow 0$  the medium can be regarded as homogeneous with higher refractive index. If the periodicity is comparable with the beam diameter, the soliton experiences maximal guiding by the lattice-induced refractive index modulation. For larger periodicity, the region in which the refractive index change is negligible increases, so that in the limit  $p \rightarrow \infty$  one ends up again with a homogeneous medium. Consequently the influence of the lattice decreases again. Furthermore, our simulations show that the decrease of the dynamics is not as rapid for smaller periodicity as it is for larger one.

Figure 3 depicts the temporal evolution of the intensity distribution for  $p = 1d$  for three different values of the lattice intensity  $A$ . For weaker lattice the output oscillates irregularly. These oscillations are similar to those occurring in a bulk continuous medium. The presence of the lattice leads to solitons residing more frequently at the lattice sites what is reflected in the appearance of faint horizontal lines in Fig. 3(a). For stronger lattice we still observe some transient dynamics with oscillation periods which are quite short [Fig. 3(b)]. During these oscillations, the output couples to the neighboring lattice sites. However, after the initial oscillations the output becomes stationary and resides at the lattice site closest to the input waveguide. For even larger lattice intensity the range of time transient dynamics shortens. Notice that in the stable



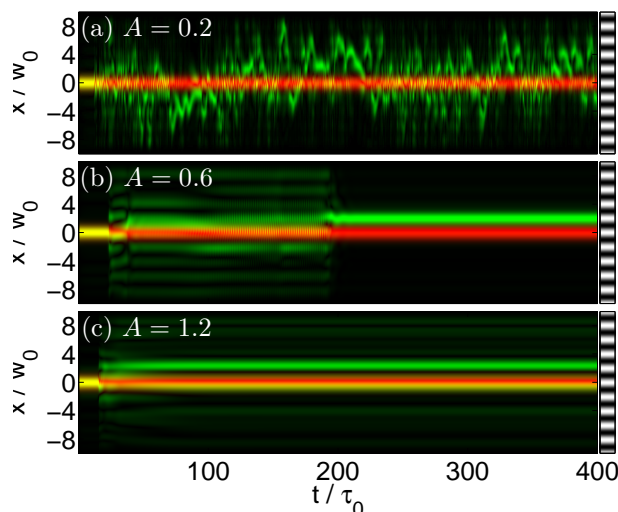


Fig. 3. Temporal evolution of the intensity distribution at one crystal face with increasing lattice peak intensity at the plane of incidence of  $F$ . The constant line (red) marks the input of  $F$  while the intensity distribution of  $B$  oscillates (green) since it is the output plane of beam  $B$ . Depicted is the evolution along the curve for periodicity equal to beam diameter. Qualitatively similar results are obtained at the plane of incidence of  $B$  for the transmitted beam  $F$ .

state a small fraction of the soliton is trapped at the input lattice channel while the majority of soliton power is confined in the neighboring site.

The intensity distribution of the stable soliton states inside the crystal depends on the periodicity and the strength of the lattice. Figure 4 illustrates the spatial intensity distributions in case of the lattice with the same strength but three different periods. The final intensity distribution results from the trade-off between the natural effect of beams trying to avoid each other and beam trapping by the lattice sites.

We saw in Fig. 2 the unexpected increase of  $lod^N$  for small period and large lattice strength. This particular case is depicted in Fig. 5(a). The increase of  $lod^N$  is caused by regular spatio-temporal oscillations of soliton beams. During these oscillations the solitons focus onto each other in the middle of the medium, then start to deflect to one side and break up. After that the sequence [as depicted in Fig. 5(b)-(d)] repeats with the spatial deflection going to the other side.

For off-site launching (i.e. the maximum soliton intensity coincides with the minimum of the lattice), the instability dynamics also decreases. However, the exact progression of the curves is somewhat different from the on-site case as depicted in Fig. 6. In general, counterpropagating solitons within this excitation scheme are more dynamic which is a result of the intrinsic dynamics due to their initial attraction of the solitons to the waveguides nearest to their point of excitation. Occasionally, an increase of the dynamics is observed for specific periodicities and low peak intensities of the lattice. As shown in Fig. 7, this increase of  $lod^N$  is due to the onset of fast oscillations. This interpretation can be explained as follows: On the one hand, the beams experience a reduction of the transverse separation of the lattice which decreases the transverse instability and leads to an increased focusing of the beams [Fig. 7 (b)]. On the other hand, the transverse separation increases the interaction region of the beams which supports the instability. In the case of beams launched off-site on lattices with low peak intensities and suitable periodicities, the complex interplay between these two effects combined with the

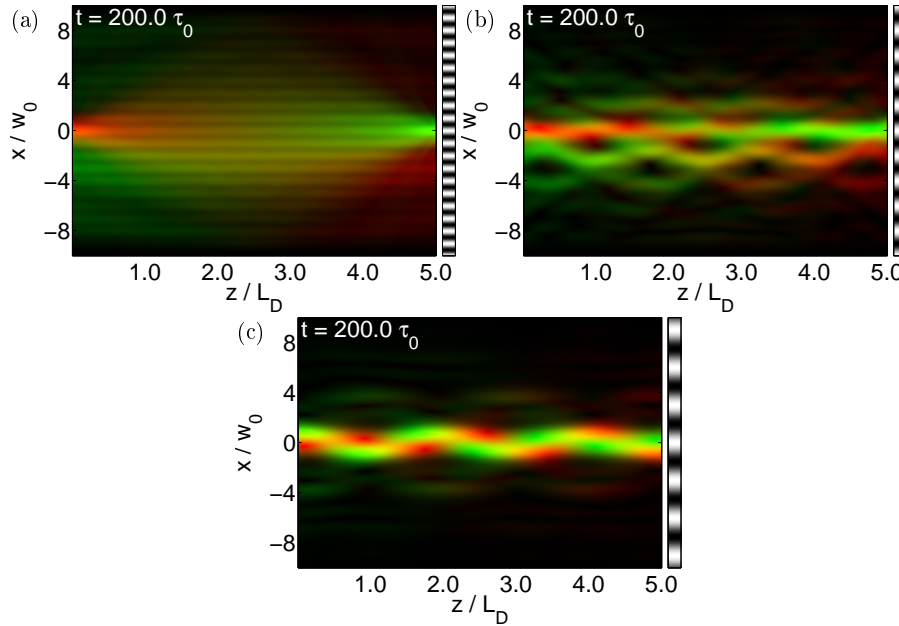


Fig. 4. Illustration of the intensity distribution for the stabilized states shown for the same lattice peak intensity of  $A = 2.4$  and periodicity of  $p = 0.5d$  in (a),  $p = 1.0d$  in (b) and  $p = 1.5d$  in (c). The blurred nature in (a) results from the mutual interaction of the solitons.

intrinsic attraction to adjacent waveguides leads to the short time scale oscillations observed in Fig. 7. Apart from this, the intensity distribution of the stabilized state inside the crystal is characterized by the combination of attraction to adjacent waveguides and avoidance of the counterpropagating beam.

### 3. Experimental stabilization of soliton dynamics

In the following section we describe results of experimental studies of the impact of an optically-induced photonic lattice on the dynamics of the soliton interaction. Following results of our numerical simulations, we investigate here the case of a lattice with periodicity comparable to the beam diameter, for which the soliton stabilization is expected to be strongest. Figure 8 shows the schematic of the experimental setup. The setup is similar to the one utilized for investigation of counterpropagating solitons [8]. A beam from a frequency-doubled Nd:YAG laser ( $\lambda = 532\text{nm}$ ) is split up into two parts with a power of  $1\mu\text{W}$  each. These beams are focussed onto the two opposite faces of the Cerium-doped Strontium Barium Niobate crystal (SBN:60) and are polarized parallel to the crystal's  $c$ -axis exploiting the large electro-optic tensor element  $r_{33}$ . They propagate through the medium slightly tilted against the crystal's  $a$ -axis ( $L = 23\text{mm}$ ) in order to compensate for beam self-bending. Both beams are made mutually incoherent by reflecting one of them from a piezo-mounted mirror oscillating with a period significantly shorter than the response time of the photorefractive nonlinearity. The SBN crystal is biased by an external DC electric field  $E_e = 1.9\text{kV/cm}$  applied along the crystal's  $c$ -axis [31]. Additionally, the crystal is illuminated by an incoherent white-light source in order to control the saturation of the nonlinearity. For synchronous observation, the transmitted and reflected beams at either crystal faces are imaged onto the same CCD camera.

In order to induce a one-dimensional photonic lattice, we launch two plane waves of equal



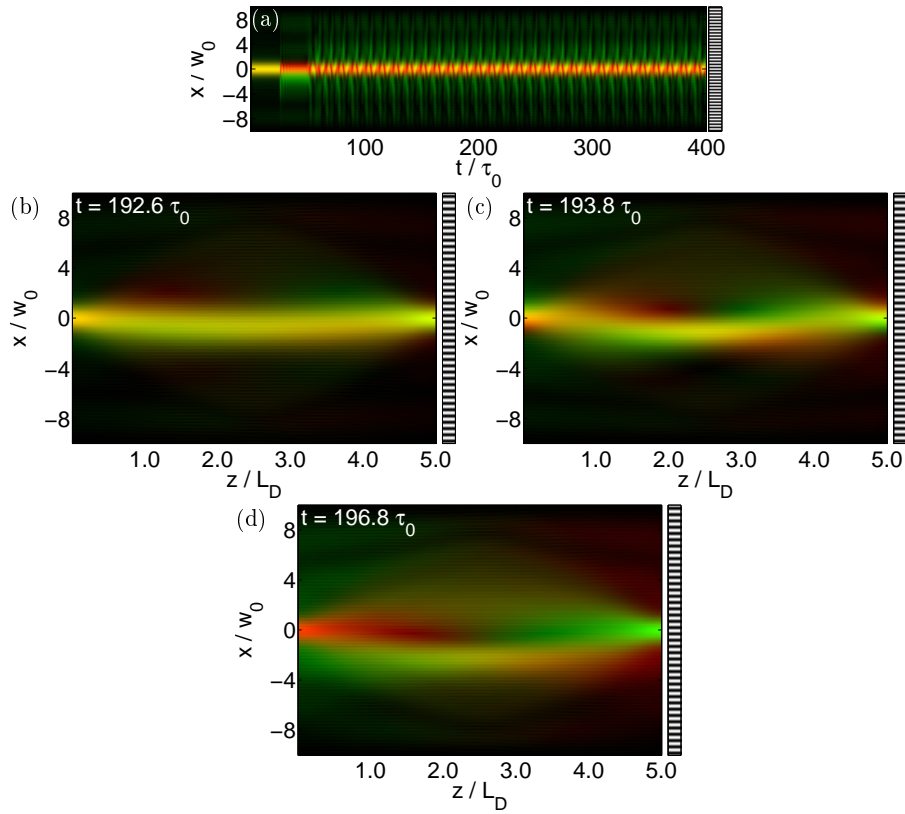


Fig. 5. Illustration of the dynamic states for  $p = 0.25d$  and  $A = 2.2$ . The temporal evolution is depicted in (a) where as (b-d) show snapshots of the oscillation comprised of sequences of focussing and deflection.

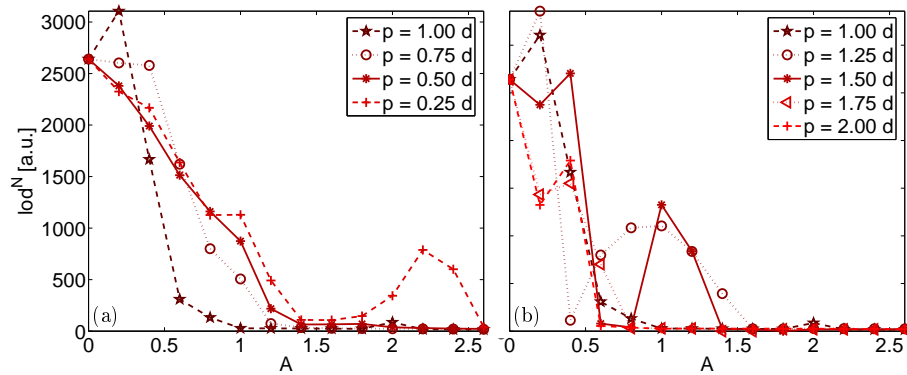


Fig. 6. Decrease in the dynamics of counterpropagating solitons launched off-site as a function of peak intensity and periodicity. (a) period smaller than the beam diameter; (b) period larger than the beam diameter.

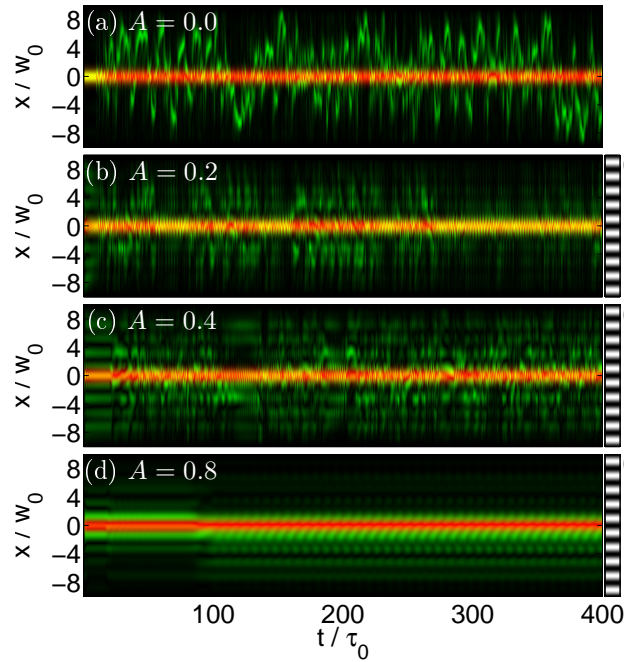


Fig. 7. Illustration of the increase of the short time scale dynamics for beams launched off-site on the lattice of periodicity  $p = 1d$ .

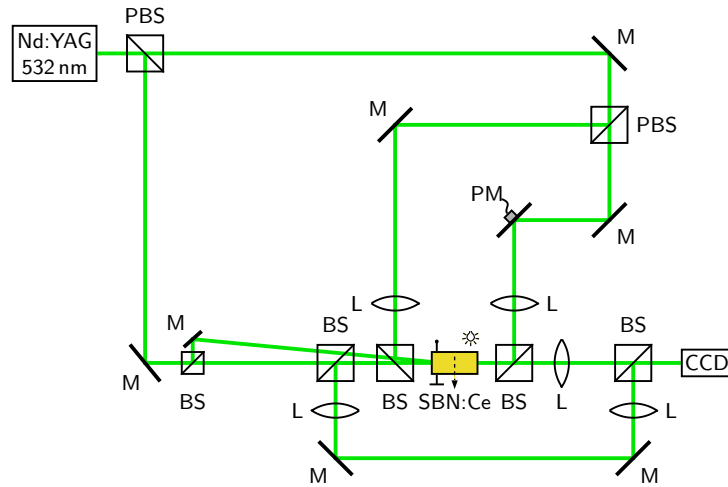


Fig. 8. Experimental setup for the observation of counterpropagating solitons on a one-dimensional lattice. MO: microscope objective, PH: pinhole, L: lens, HWP: half wave plate, M: mirror, PBS: polarizing beam splitter, PM: piezo-mounted mirror, BS: beam splitter

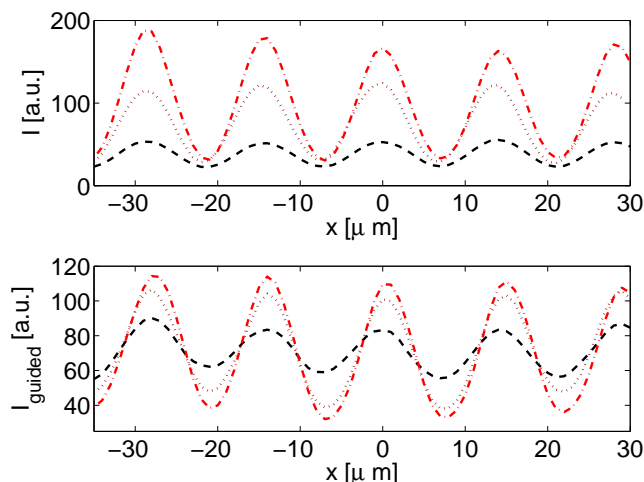


Fig. 9. Comparison between the modulation of the interference pattern (top) and the induced refractive index modulation (bottom) measured in terms of the intensity modulation of a guided plane wave. Shown are the results for lattice wave powers of 0.5mW (dashed line), 1.5mW (dotted line) and 2.5mW (dash-dot line).

power that interfere inside the photorefractive crystal. Due to their ordinary polarization, the lattice waves do not experience the refractive index modulation induced by themselves and the solitons. Thus they effectively propagate in a linear regime and write a stationary (in propagation variable  $z$ ) refractive index modulation. The lattice peak intensity is adjusted by varying the power of the two interfering waves. Figure 9 compares the intensity of the interfering beams with the modulation of a guided plane wave used as a tool for characterization of the refractive index modulation.

Our experimental results are shown in Fig. 10 which depicts temporal evolution of one of the beam at the exit face of the crystal. It is evident that soliton dynamics, i.e. spatio-temporal oscillations are suppressed with the increasing strength of the optical lattice. These results agree qualitatively well with our numerical simulations. Figure 10(a) shows irregular oscillations appearing at low lattice strength. These oscillations are comparable to those emerging in a bulk medium under the same set of parameters. For higher power of the lattice forming beams [Fig. 10(b,c)] the oscillations amplitude starts to decrease and sequences of regular oscillations appear. For even higher power of the lattice waves we see long lasting transient dynamics tending to a stationary state [Fig. 10(d)]. Finally, a stationary state over the observation period of two hours is seen for lattice beam power of 2.5mW [see Fig. 10(e)].

This evolution is accompanied by an increased trapping of light in neighboring lattice sites. The asymmetry of trapping in the lattice channels is due to the beam-bending effect. Due to the change in the refractive index, the self-bent soliton gets partially reflected when it passes a lattice site and the reflected light travels along the waveguide written by the lattice wave. Moreover, the weaker oscillations in  $y$ -direction are suppressed with increasing lattice peak intensities.

It is worth noting, that the experimental stabilization of counterpropagating solitons has been achieved with lattice strengths much lower than that found in numerical simulations. For instance the experimental case of lattice power of  $A = 2.5\text{mW}$  corresponds to  $A = 0.05$  which is significantly lower than 0.60 necessary to stabilize the solitons in numerical simulations.

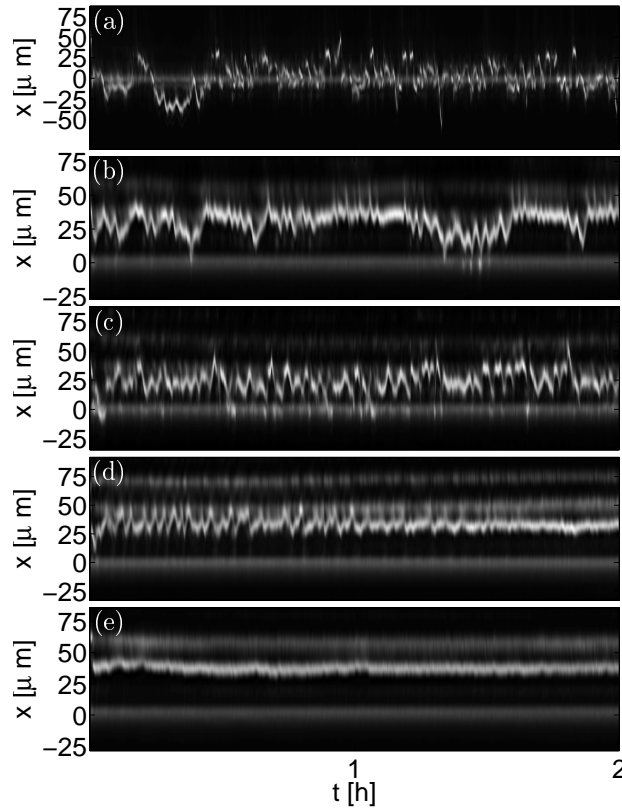


Fig. 10. Temporal evolution of the intensity distribution projected onto the  $x$ -axis (parallel to the  $c$ -axis) for different lattice powers of (a)  $250\mu\text{W}$ , (b)  $1.0\text{mW}$ , (c)  $1.5\text{mW}$ , (d)  $2.0\text{mW}$ , and  $2.5\text{mW}$ . The faint horizontal lines at  $x = 0\mu\text{m}$  mark the reflected beam at this crystal face which acts as a reference. Again the results for the other crystal face show similar behaviour.

#### 4. Soliton stabilization in two-dimensional photonic lattices

So far we have considered the dynamics of counterpropagating solitons in a 1D lattice, emphasizing the arrest of instability in a single transverse direction only. For application of the counterpropagating solitons as a self-adjusting bi-directional waveguide, it is necessary, however, to ensure stabilization in both transverse directions. This can be achieved in two-dimensional optical lattices. To this end, in our experiments we used a 2D square lattice, oriented under  $45^\circ$  with respect to the crystalline axis [Fig. 11(a)] similar to Refs. [40,41]. Such orientation of the lattice is preferable in order to reduce the effect of the intrinsic anisotropy of the photorefractive non-linearity [42]. We then vary the lattice period and power and monitor the positions of the beams at both faces of the crystal. The inputs of the forward and the backward propagating beams in our experiments have the size of  $19\mu\text{m}$  and  $18\mu\text{m}$ , respectively [Fig. 11(b)]. In our 10 mm long crystal this corresponds to approximately 5 diffraction lengths of linear propagation.

First we studied dependence of beam dynamics on the lattice period. Our experimental results qualitatively matched those obtained for 1D optical lattice. For a small lattice period ( $3\mu\text{m}$ ) the potential induced by the lattice was too weak to arrest the instability of the counterpropagating beams. With the increased lattice period (to 6, 9, or  $12\mu\text{m}$ ) the instability was practically removed for a certain range of lattice strength. The large lattice periods, however, strongly reduce

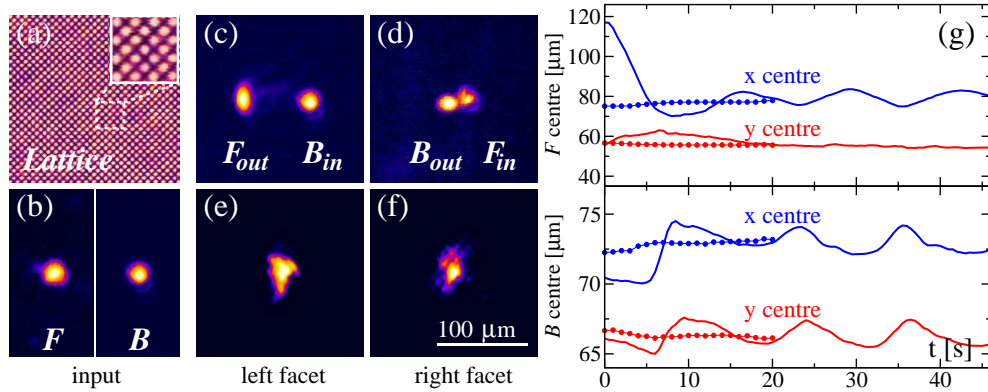


Fig. 11. Stabilization of the instability in two transverse directions: (a) 2D square lattice of  $6\text{ }\mu\text{m}$  period. (b) Input intensity distribution for the forward ( $F$ ) and backwards ( $B$ ) propagating beams, respectively. (c,d) Digitally combined beam profiles at the left and right face of the crystal when each soliton propagates independently. (e,f) Stabilization on the lattice for both faces of the crystal, respectively. (g) Position of the output beams center without the lattice (solid line) and with the lattice (dotted line) as a function of time.

the mobility of the beams as each beam can be fully trapped in a single lattice site. Such trapping imposes a constrain on the formation of bi-directional waveguide which becomes sensitive on the initial alignment of the beams. Thus, beams propagating in different directions inside the crystal will not attract, as their intensity overlap will be reduced by the trapping on different lattice sites. Therefore, in the following experiments we concentrated on the intermediate case of a lattice of period  $6\text{ }\mu\text{m}$  ( $p = 0.3d$ ).

Without the lattice, both beams overlap weakly and their individual propagation is strongly affected by the beam self-focusing and self-bending. At bias electric field of  $2\text{ kV/cm}$  and at powers of  $1\text{ }\mu\text{W}$  each beam forms a spatial soliton, where the soliton size is equal to the input beam size. In Fig. 11(c,d) we show the digitally combined input and output of each beam as if they would propagate without interaction inside the crystal. When both beams co-propagate they start to interact. After the initial attraction, the beams exhibit oscillatory dynamics. The oscillations are depicted in Fig. 11(g, solid line) showing the  $(x,y)$  position of the output beam center of mass as a function of time. In this experiment we first established the soliton formation of the backward beam  $B$  and then we launched the forward propagating beam  $F$ . The observed oscillatory dynamics is similar to the 1D case, but appears in both transverse directions. The amplitude of the oscillations is dependent on the initial alignment of the beams.

The introduction of the lattice suppresses the oscillatory instability observed in homogenous crystal due to the induced periodic potential and therefore reduced mobility of solitons. In our experiments, we first established an unstable bi-directional soliton state and afterwards we launched the lattice beams. The lattice power was  $2.8\text{ mW}$ , resulting in approximately 5 times lower intensity than that of the soliton. In the presence of the lattice both beams align well with each other [Fig. 11(e,f)] and the oscillatory motion is suppressed as shown in Fig. 11(g, dotted line). Furthermore, we monitored the long term ( $\sim 1\text{ hour}$ ) dynamics of the beams on the lattice and observed that small variations of the beam position can still be seen, however, these variations were rather weak as compared to the case when the lattice is absent.

In the next step, we investigated the dependence of the beam dynamics on the lattice strength. As expected, for stronger lattices the instability dynamics of the counterpropagating beams is reduced and the solitons join steadily at both sides of the crystal. At lattice power higher than

3.2 mW, however, the forward and backward propagating beams start to significantly increase their output size as a result of the increased effective background illumination and reduced self-focusing. Therefore, an optimal lattice power can be obtained (2.8 mW in our experiments) at which the beams are well localised and the dynamic instability is strongly suppressed.

## 5. Conclusion

In conclusion, we studied the impact of an optically-induced photonic lattice on the dynamics of counterpropagating solitons in a biased photorefractive crystal. Our numerical simulations demonstrate that an optically-induced lattice of proper period and strength can suppress and even completely arrest the instability. We found that counterpropagating solitons launched on-site as well as off-site can be stabilized. In the case of small periodicity and high peak intensity of the lattice, we observed unexpected spatio-temporal oscillations with characteristics dissimilar from those exhibited by counterpropagating solitons in bulk media. We demonstrated experimentally the decrease of dynamics for a one-dimensional lattice with periodicity comparable to the beam diameter. The temporal evolution of the intensity distribution was found to be in good qualitative agreement with our numerical results. Additionally, the stabilization of the counterpropagating soliton dynamics was demonstrated for two-dimensional square lattices, allowing for stability of the induced bi-directional waveguide in two transverse directions.

Based on our observations, novel schemes to control the dynamics of counterpropagating solitons are possible. These schemes may also be applicable to other field of physics since our numerical simulations show a decrease of instability dynamics for a quite general model including a saturable Kerr-like nonlinearity.

## Acknowledgements

The authors acknowledge fruitful discussions with Bernd Terhalle and thank him for his technical support.